Journal of Robotics and Control (JRC)
Volume 5, Issue 6, 2024
ISSN: 2715-5072, DOI: 10.18196/jrc.v5i6.23120

Overvoltage and Oscillation Analysis for a Full-Bridge Isolated DC-DC Converter

Boris A. Avdeev [1], Aleksei V. Vyngra [2], Anton A. Zhilenkov [3], Sergei G. Chernyi [4*], Andrey Degtyarev [5], Aleksandr Kustov [6] Anton Zinchenko [7]
[1, 2] Kerch State Maritime Technological University, Kerch, Russian Federation
[3, 4, 5, 6, 7] St. Petersburg State Marine Technical University, St. Petersburg, Russia
Email: [1] dirigeant@mail.ru, [2] elag1995@gmail.com, [3] zhilenkovanton@gmail.com, [4] sergiiblack@gmail.com, [5] capitanandreydegtyerev@gmail.com, [6] kustov@smtu.ru, [7] antel85@bk.ru
*Corresponding Author

***Abstract*—The paper deals with determining and eliminating overvoltage's and ripples from the output of a high-frequency inverter bridge in a full-bridge DC converter. These oscillations can cause overvoltage on the elements of the power converter, which in turn can lead to false triggering of semiconductor keys or their failure. Schematic diagrams of the bridge are given; the principle of its operation is described. A simplified equivalent circuit replaces the classic bridge. A qualitative analysis of transient processes in the resulting scheme is made. The voltage at the output of the bridge is found using the operator method. The findings have been compared with the simulation model executed in MATLAB/Simulink. The presented method is less labor-intensive than simulation modeling and allows for faster and easier verification of the permissible overvoltage level and oscillation frequency, which is especially important in devices containing a large number of nonlinear elements. It is shown how the parameters of the bridge affect the performance of the transient, in particular the overshoot and oscillation frequency. The attained dependencies are shown in graphical form. The ways of improving the quality of the transition process are given. The findings have been verified on an experimental setup. The obtained theoretical results are consistent with the results of the experiment with the data of other researchers.**

Keywords—DC-DC Converter; Surge Voltage; Transient Response; Snubber Circuit.

I. INTRODUCTION

Devices such as a double active bridge, a full bridge converter or a solid state transformer consist of fairly well-researched blocks, both in terms of operation of the nodes and in terms of their control. However, research in these areas is ongoing and intensive. The problem lies in the compatibility and reliability of the performance of different elements in respect of each other [1]-[10]. The complexity is added by the fact that the above devices consist of semiconductor elements, and they are all non-linear, so it is difficult to apply classical calculation methods. Another problem is that it is difficult to take into account noise caused by switching processes in power switches when modeling.

II. OBJECTIVE AND LITERARY REVIEW

The objective of this research is to determine the output overvoltages and ripples from the single-phase bridge output, and to determine the influence of the bridge parameters on the transient performance. The findings will be used in further studies to calculate the operation and determine the reliability of a full-bridge converter. Moreover, they will also serve as a basis for calculating the optimal design of the snubber chain.

A schematic diagram of a full-bridge converter is shown in Fig. 1. Power is supplied from a GB DC source to a bridge consisting of 4 semiconductor switches S1-S4. Control signals are applied to the bridge in such a way that a three-level signal is observed at the output of the bridge. The bridge's output connects to the primary winding of a high-frequency transformer (TV). In cases where the self-inductance of the transformer is small, it is required to add an auxiliary inductance L in series with the transformer in order to achieve better power transfer control. The voltage at the output of the RF transformer TV is rectified using an uncontrolled rectifier based on diodes VD1-VD4. Capacitors C1 and C2 serve in order to smooth the voltage at the input and output, respectively.

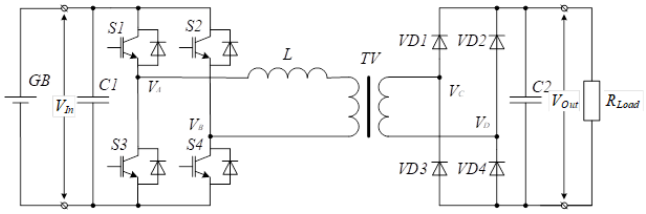

Fig. 1. Full bridge converter

When the power switch of the converter secondary (output) side is closed, a step voltage is generated, approximately 2 times higher than the reverse applied voltage of the diode [2]-[5]. Therefore, in the case of an input voltage with a value equal to the average level (380-400 V); the power semiconductor switch must withstand a voltage of at least 2000 V. With this value of the reverse voltage, the size and cost of semiconductor elements increases. As a measure to counteract overvoltage, various damping schemes (snubbers) are used. Overvoltage collector-emitter breakdown is one of the most common causes of transistor converter failure. In practice, high slew rates are often deliberately slowed down by adding drain-gate capacitance to prevent excessive EMI, although at the cost of some loss in conversion efficiency [3][4]-[8]. The damping and voltage limiting effect of the snubber is achieved by diverting energy into the capacitor in the circuit and slowing down the rate of rise of the voltage front. It can also serve to reduce dynamic switching losses by separating current and voltage overlap in

a "hard" switching converter, reducing the resulting high dissipation transients.

There are a large number of damping schemes [5][6]. The basis of almost all damping circuits are capacitors, which, according to the second switching law, smooth out the voltage rise front, thereby limiting it. Snubber circuits can also include inductors and resistors. At high converter powers, snubber circuits become bulky [7]-[15]. For example, damping resistors require a large amount in order to dissipate the heat.

Before developing methods for suppressing overshoot, it is necessary to investigate the transient process during switching. Let us calculate the transient process when changing the polarity of the output of the power bridge [14]-[18].

The bridge operates into a transformer, which is an active-inductive load. Schematic diagrams of the bridge operation are shown in Fig. 2. Neglecting the dead time, two states of the bridge can be distinguished. They are as follows: current flow in the load in the forward direction (cycle 1) and in the reverse direction (cycle 2). The contours of the current flow in each circuit in the steady state are highlighted in red.

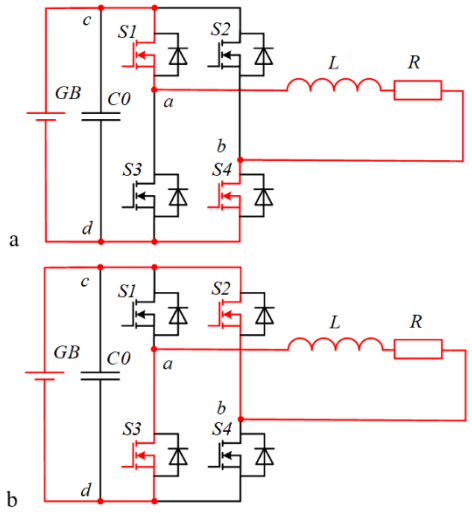

Fig. 2. Operation of the bridge into the active-inductive load

III. MATHEMATICAL MODELING

The bridge is powered either by a laboratory programmable linear DC supply or by a mains-powered rectifier or transformer. In any case, a real voltage source has inductance. The transistor has a small parasitic capacitance, so we will replace the transistor in the open state with a resistor equal to the resistance in the open state and a capacitor connected in parallel equal to the parasitic capacitance. It is also desirable to take capacitance into account. It is required to consider the snubber in the form of a capacitance installed on the key, as the most common option for implementing soft switching. The current through the transistor will be the sum of the current through the resistor and capacitor [17]-[20].

In order to avoid cumbersome and complex formulas, let solve the problem numerically. To do this, set the following schema parameters: input voltage E=100 V, voltage source inductance L_0=1 μH, voltage source resistance R_0=0.1 Ω, input capacitor capacity C_0=0.1 μF, transistor on-resistance R_{on}=0.27 Ω, parasitic capacitance of a transistor C_d=450 nF, load resistance R=10 Ω, load inductance L=5 μH.

Let us make a qualitative analysis of transient processes. Calculation of currents and voltages before switching (t=0-).

The complexity of the calculation lies in the fact that the circuit does not have a switching device in the classic sense. Also, the current before switching and after switching flows through different transistors [20]-[23].

$$I_1(0\_) = -I_3(0\_) = I`_4(0\_) = I`_5(0\_) = \frac{E}{R_0 + R_{on1} + R_{on4} + R} = 9.398A$$

where $I`_4$ and $I`_5$ are currents in opposite transistors, A; R_{on3} and R_{on4} are resistances of opposite transistors in the open state, Ω.

$$I_2(0\_) = 0A$$

$$V_C(0\_) = I_1(0\_)(R_{on1} + R_{on4} + R) = 99.06V$$

The scheme in the steady state is shown in Fig. 3. Calculation of currents and voltages in steady state

$$I_{1st} = I_{3st} = I_{4st} = I_{5st} = \frac{E}{R_0 + R_{on2} + R_{on3} + R} = 9.398A,$$

$$V_{Cst} = V_C(\infty) = I_{1st}(R_{on2} + R_{on3} + R) = 99.06V,$$

$$V_{4Cst} = V_{4C}(\infty) = I_{4st}R_{on1} = 2.538V,$$

$$V_{5Cst} = V_{5C}(\infty) = I_{5st}R_{on2} = 2.538V.$$

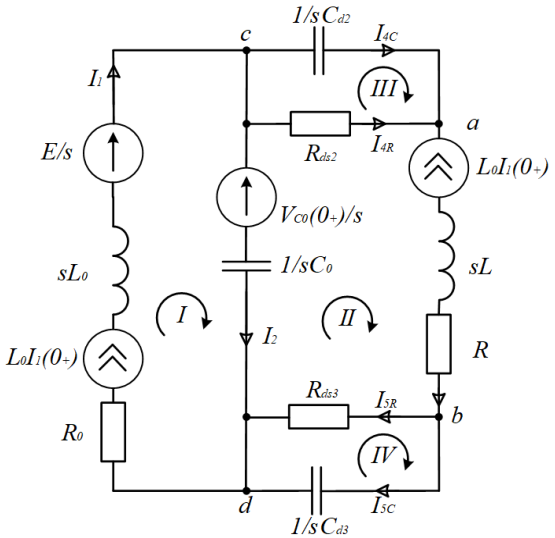

Fig. 3. Operator equivalent circuit of the post-commutation circuit

Let us consider the transient process when changing the polarity in further detail. To do this, we calculate the transient process by the operator method. The advantage of the operator method for calculating transient processes is the lower labor intensity of calculating complex circuits compared to the classical method. The operator method is based on transferring the calculation of the transient process from the area of functions of a real variable (time t) to the area of functions of a complex variable (or operator variable), in which differential equations are transformed into algebraic ones. The operator equivalent circuit of the post-switching circuit is shown in Fig. 4. The coil is replaced by a series-

connected operator resistance sL_0 and a voltage source $LI_1(0_+)$, where $I_1(0_+)$ is the value of the current in the inductance at $t = 0+$. The capacitor is replaced by series-connected operator resistance $1/sC_0$ and voltage source $V_{c0}(0_+)/s$, where $V_{c0}(0_+)$ is the value of the voltage across the capacitance at $t = 0_+$. The direction of the source $LI_1(0)$ coincides with the direction of the branch current, and the direction of the source $V_{c0}(0_+)/s$ is opposite to the current in this branch [24]-[27].

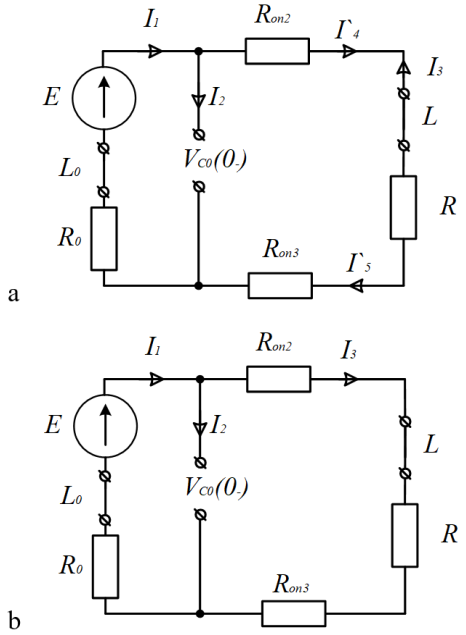

Fig. 4. Scheme at time t=0- and in steady state

Compose a system of equations according to Kirchhoff's laws. According to Kirchhoff's first law:

$$\begin{matrix} a) \\ b) \\ c) \end{matrix}\begin{cases} I_{4R} + I_{4C} - I_3 = 0 \\ -I_{5R} - I_{5C} + I_3 = 0 \\ -I_2 - I_{4R} - I_{4C} + I_1 = 0 \end{cases}$$

From Kirchhoff's second law:

$$\begin{matrix} I) \\ II) \\ III) \\ IV) \end{matrix}\begin{cases} I_1(R_0 + L_0 s) + I_2 \dfrac{1}{C_0 s} = \dfrac{E}{s} + I_1(0_+)L_0 - \dfrac{V_{C0}(0_+)}{s} \\ -I_2 \dfrac{1}{C_0 s} + I_{4R}R_{on2} + I_{5R}R_{on3} = \dfrac{V_{C0}(0_+)}{s} - I_3(0_+)L \\ I_{4C}\dfrac{1}{C_{d2}} - I_{4C}R_{on2} = 0 \\ I_{5C}\dfrac{1}{C_{d3}} - I_{5C}R_{on3} = 0 \end{cases}$$

Let us find $I_3(s)$:

$$I_3(s) = -\frac{1.142s^4+7.106s^3-9.979s^2+4.891s-2\cdot10^{48}}{1.215\cdot10^{25}s^5+1.255\cdot10^{28}s4+3.69e^{34}s^3+1.4666e^{41}s^2+2.12\cdot10^{47}s}.$$

The easiest way to find the original of this expression is to use the Heaviside expansion formula:

$$V_{ab}(t) = \sum_{k=1}^{m} \frac{N(s_k)}{M'(s_k)} e^{s_k t},$$

where k is a number of number of roots of the characteristic equation $M(s) = 0$. Find the roots of the denominator $M(s) = 0$:

$$s\left(1.215s^4 + 1.256\cdot10^7 s^3 + 3.69\cdot10^{13}s^2 + 1.467\cdot10^{20}s + 2.128\cdot10^{26}\right) = 0,$$

$$s_0 = 0;$$
$$s_1 = -8.089\cdot10^6;$$
$$s_2 = -1.874\cdot10^6;$$
$$s_3 = -1.837\cdot10^5 - 3.394\cdot10^6 j;$$
$$s_4 = -1.837\cdot10^5 + 3.394\cdot10^6 j.$$

Omitting the intermediate results in accordance with the Heaviside expansion formula, we obtain the desired function of the current time $I_3(s)$:

$$I_3(t) = 9.398 + 0.265\,exp(-8.089\cdot10^6 t) - 17.662\,exp(-1.874\cdot10^6 t) + 2.593\,cos(3.394\cdot10^6 t - 57.307°)\,exp(-1.837\cdot10^5 t).$$

The resulting value is shown in Fig. 5 a. Find the voltage at the output of the bridge:

$$U_{ab}(s) = I_3(s)\cdot(R + Ls) = \frac{11.419s^4 + 7.106\cdot10^7 s^3 - 9.978\cdot10^{13}s^2 + 4.891\cdot10^{20}s - 2\cdot10^{27}}{1.215s^5 + 1.256\cdot10^7 s^4 + 3.69\cdot10^{13}s^3 + 1.467\cdot10^{20}s^2 + 2.128\cdot10^{26}s}.$$

In accordance with the Heaviside expansion formula, we obtain the desired function of the voltage time at the output of the bridge:

$$V_{ab}(t) = 93.985 - 8.077\,exp(-8.089\cdot10^6 t) - 11.163\,exp(-1.874\cdot10^6 t) + 49.91\,cos(3.394\cdot10^6 t - 60.884°)\,exp(-1.837\cdot10^5 t).$$

The resulting value is shown in Fig. 5 b. Current overshoot does not exceed 17%, while voltage overshoot is 42%. Considering that the safety factor used when selecting the nominal values of the element base is 1.1-1.4, there is a probability of transistor breakdown. Therefore, to select the voltage, it is necessary to pre-calculate the current and voltage oscillations.

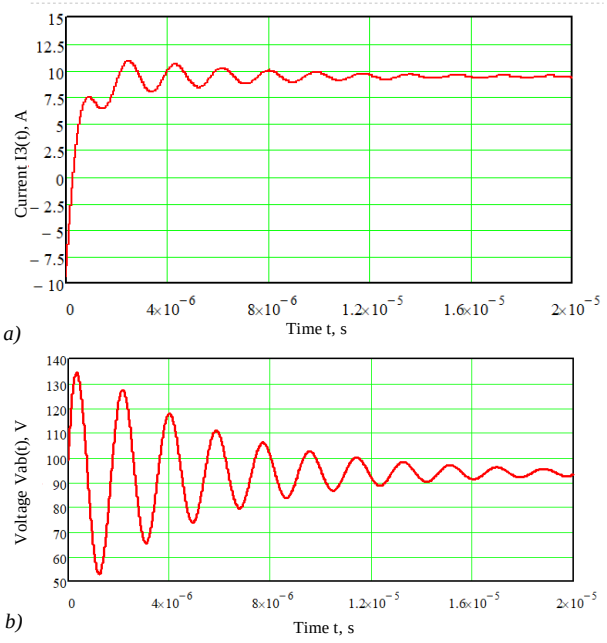

Fig. 5. Transients of current (a) voltage (b) at the output of the bridge

This calculation can be adapted not only for bridge converters and dual active bridges, but also for LLC, LCC and others resonant converters, as well as for wireless power transmission systems.

IV. Simulation Results

To check the robustness of our estimates for the transient process, we will simulate the circuit shown in Fig. 3 in Matlab/Simulink [23]-[30]. The simulation model is shown in Fig. 6(a), voltage oscillogram - in Fig. 6(b), current one - in Fig. 6(c).

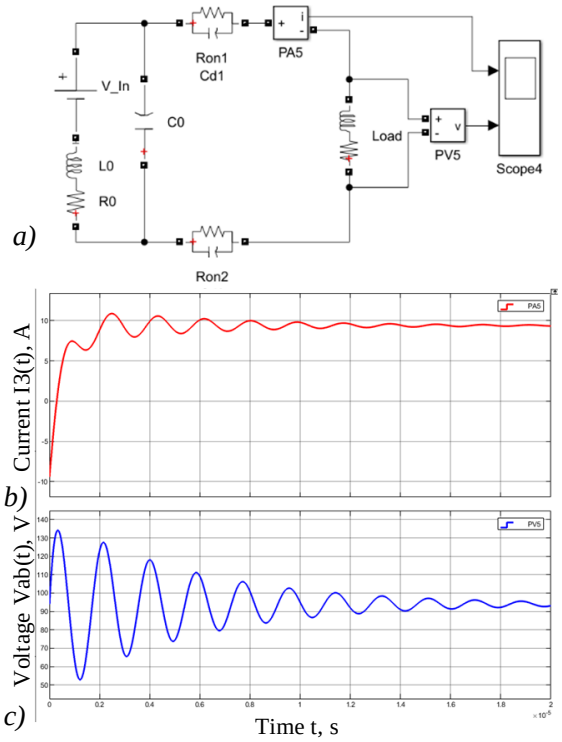

Fig. 6. Simulation model for calculating the transient process; a) electric circuit; b) voltage oscillogram; c) current oscillogram

Simulation results in Fig. 4 and Fig. 6 are completely identical, which proves the accuracy of the calculations made. Compare with simulation of a real power bridge circuit. The simulation model is shown in Fig. 7(a), voltage oscillogram - in Fig. 7(b), current oscillogram - in Fig. 7(c).

Simulation results in Fig. 6 and Fig. 7 coincide, the correlation coefficient R^2=0.97. That confirms the robustness of the equivalent circuit for the calculation.

Thus, it is possible to estimate the approximate ripple during the operation of a single-phase bridge converter. The active resistance at the output of the bridge is determined by the sum of the active resistance of the auxiliary inductor, the active resistances of the primary and secondary coils of the high-frequency transformer, the on-state resistances of the rectifier and the active load [25]-[31]. The inductance at the output of the bridge is determined by the sum of the inductive reactance of the auxiliary inductor, the inductive reactance of the primary and secondary coils of the high-frequency transformer. It should be noted that the smoothing inductance after the output rectifier does not affect the ripple in the bridge converter, being fully confirmed experimentally.

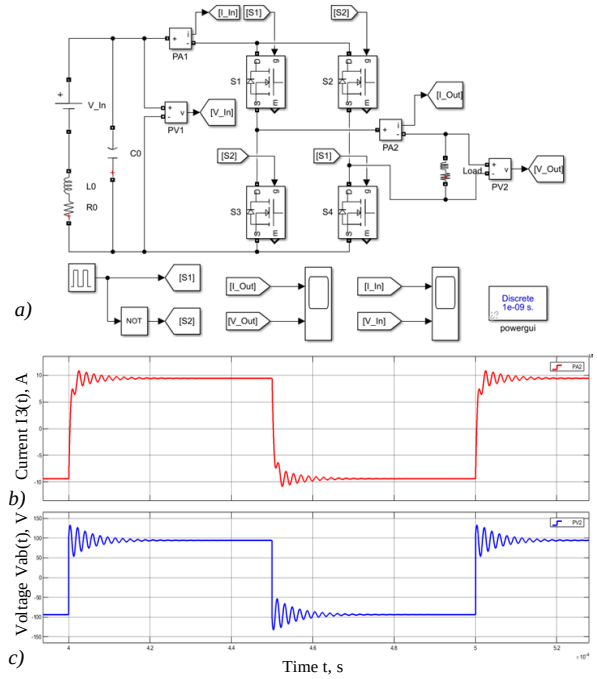

Fig. 7. Power bridge simulation model; a) electrical diagram; b) voltage oscillogram; c) current oscillogram

Fig. 8 shows the dependency that reflects the relationship between overshoot and inductance at the output of the bridge and the capacitance of the smoothing capacitor at the input.

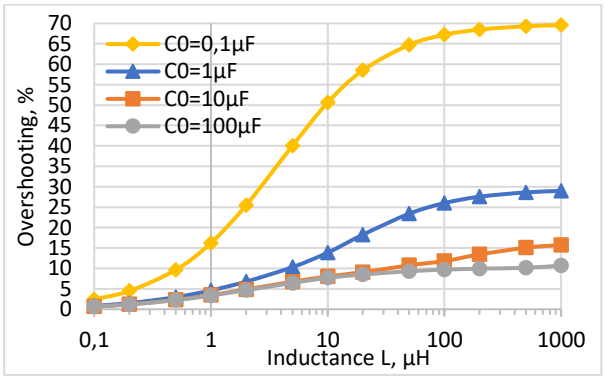

Fig. 8. The dependence of the overshoot of oscillations on the inductance at the output of the bridge and the capacitance of the smoothing capacitor at the input

As one can see from Fig. 8, with a step-up in the inductance at the output of the bridge, the voltage overshoot increases. However, this is observed only up to a certain level. For this case, the value of 100 μH is the limit value, after which no increase in overshoot is observed. The oscillation frequency does not depend on the inductance and is $501kHz$, $159kHz$, $50kHz$ and $14kHz$ for an input capacitance of 0.1 μF, 1 μF, 10 μF and 100 μF, respectively.

Fig. 9(a) shows the dependence of overshoot and oscillation frequency on the input capacitor for different values of the output inductance. Obviously, with an increase in the input capacitance, the overshoot decreases, which is confirmed by various independent studies on electromagnetic compatibility [8], [9], [10], [32]-[40]. However, there is no point in increasing the input capacitance to infinity, trying to remove the overshoot completely. The presence of overshoot

is due not only to transient processes in the capacitor, but it also depends on other reactive elements of the electrical network. It can be seen from the graph that at $C = 10\ \mu F$, the overshoot remains practically unchanged even with a high output inductance. It means that it makes no practical sense to install an oversized capacitor to improve the transient. As it was mentioned above, the ripple frequency does not depend on the output inductance, which is confirmed by Fig. 9(b). The relationship between $lg(C0)$ and $lg(f)$ is linear and despite some differences in the frequency data for different values of L, the root mean square correlation is 99.85%.

The input inductance value has almost no effect on transient overshoot (Fig. 10(a)), but reduces the ripple frequency (Fig. 10(b)). The missing part of the line on the second graph indicates that the process is astatic and there are no oscillations in it.

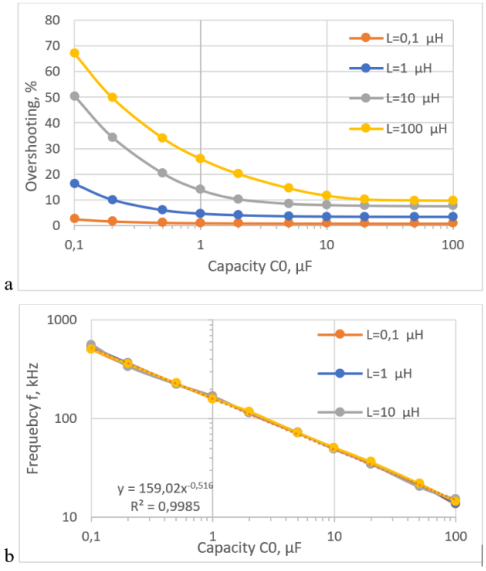

Fig. 9. Dependence of overshoot (a) and oscillation frequency (b) on the input capacitor at different values of the output inductance

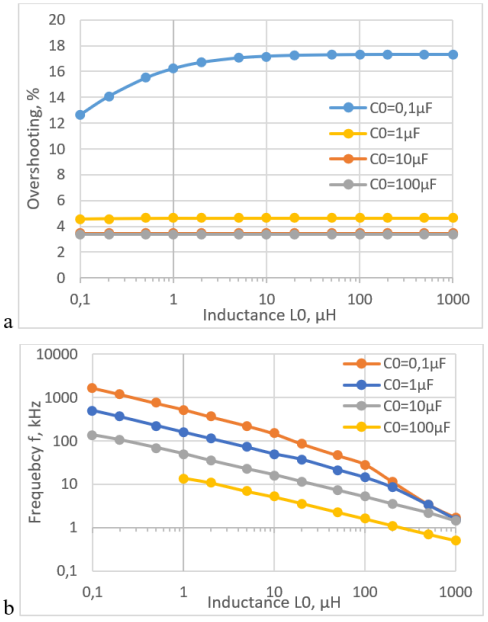

Fig. 10. Dependence of overshoot (a) and oscillation frequency (b) on the input inductance for different values of the input capacitor

V. EXPERIMENT

To verify the data produced theoretically, an experiment was carried out with a laboratory full-bridge converter, shown in Fig. 11. The inverter is assembled from four IRF730PBF, rated at 400V and 5.5A. The KBU1010 diode bridge is rated for 10A and 1000V. Input capacitor: 1000uF, 400V; output capacitor: 100uF, 400V. The number of turns on the primary and secondary windings of the transformer is 100 and 50, respectively [41]-[50]. The M2500NMS1 ferrite ring core with dimensions 40×25×11 acts as a magnetic circuit. The control was carried out using the STM32F407G-DISC1 debug board based on 32-bit ARM Cortex-M4 microcontrollers. The pulse generation frequency is 5 kHz. The load factor is maximum, it being almost 50%. The dead (insensitive) time was 1 μs.

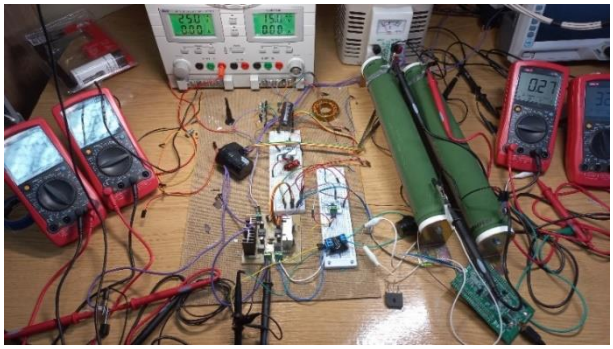

Fig. 11. Experimental installation to research a full-bridge converter

Replacing the capacitance of the input capacitor, the voltage oscillograms from the output of the bridge were obtained, shown in Fig. 12. As it can be seen from Fig. 12 voltage surges with polarity reversal are 10%, 22% and 117%. In the latter case, overshooting can lead to overvoltage on semiconductor switches and subsequent burnout of the element. The theoretical overvoltage values are 8.78%, 17.54%, and 87.23%. Despite the high error in the latter case, in general, theoretical data make it possible to approximately estimate the strength of oscillations that occur during the operation of a full-bridge converter. Moreover, the team of authors fully recognizes the fact that the real situation with the transient process is much more complicated than that presented in this paper. It does not negate the fact that these dependencies take place, being suitable for indirect assessment of the transient process.

The issue of the influence of snubber chains connected in parallel has been raised in the scientific literature more than once [11][12][51]-[60]. Theoretical dependencies and experimental studies showing reductions in overshoot are completely consistent with those carried out earlier and do not add anything new to this consideration. However, the use of these mathematical and simulation models will allow us to select the optimal design and parameters of damper chains.

The results obtained can be applied by engineers working with full-bridge converters in the design of renewable energy systems, smart energy, smart grid, wireless charging or electric vehicles and will provide smoother switching of transistors, which will reduce overvoltage on elements, electrical ringing and improve electromagnetic compatibility [61]-[70].

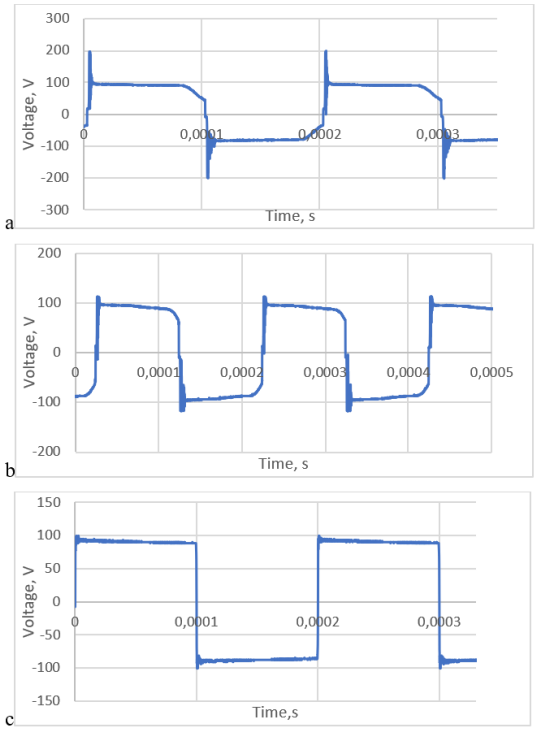

Fig. 12. Voltage oscillograms from the bridge output at a) C0=1 μF; b) C0=10 μF; c) C0=100 μF

VI. CONCLUSION

The presented theoretical calculations and schemes allow us to formulate the following dependencies for full-bridge converters; 1) The input inductance does not affect the overshoot, however, as the inductance increases, the oscillation frequency decreases. 2) Increasing the input capacitance reduces overshoot and oscillation frequency. 3) The output inductance does not affect the oscillation frequency, but as it increases, the overshoot increases.

The application of the produced dependences and the mathematical description of transient processes will make it possible to determine the reliability of a full-bridge converter and calculate the optimal snubber chain design for a wide range of device component base.

Moreover, based on the dependences produced by mathematical description, modeling and experiment, it should be concluded that the use of semiconductor power switches as part of a full-bridge converter may compromise device efficiency of the device [71]-[80]. The addition of snubber circuits, input and output inductances increases the reliability of the circuit in terms of reducing overvoltages and reducing the likelihood of breakdown of power switches, while sacrificing the efficiency of the converter itself. Further studies by the authors will be devoted to finding the most optimal parameters of the converter control system to achieve the highest efficiency of the device.

FUNDING

The research is partially funded by the Ministry of Science and Higher Education of the Russian Federation as part of the World-class Research Center program: Advanced Digital Technologies (contract No. 075-15-2022-312 dated 20 April 2022).

REFERENCES

[1] B. Avdeev, A. Vyngra, and S. Chernyi, “Improving the Electricity Quality by Means of a Single-Phase Solid-State Transformer,” *Designs*, vol. 4, no. 3, p. 35, 2020, doi: 10.3390/designs4030035.

[2] K. Domoto *et al.*, “Surge Analysis and Snubber Design for a Full-Bridge Isolated DC-DC Converter in HVDC Power Distribution Systems,” *IEEJ Transactions on Industry Applications*, vol. 133, pp. 1171-1178, 2013, doi: 10.1541/ieejias.133.1171.

[3] H. Hizarci, K. Kalayci, O. Demirel, and U. Arifoğlu, “Reducing Electromagnetic Interference in Three-Level T-type Isolated Bidirectional DC-DC Converter Using a Snubber Circuit,” *International Journal of Applied Mathematics Electronics and Computers*, vol. 9, pp. 26-34, 2021, doi: 10.18100/ijamec.934394A.

[4] D. Nair, K. Prasad, and T. Lie, “Implementation of Snubber Circuits in a PV-Based Off-Grid Electric Vehicle Charging Station—Comparative Case Studies,” *Energies*, vol. 14, p. 5853, 2021.

[5] A. Blinov, I. Verbytskyi, D. Peftitsis, and D. Vinnikov, “Regenerative Passive Snubber Circuit for High-Frequency Link Converters,” *IEEE Journal of Emerging and Selected Topics in Industrial Electronics*, 2021, doi: 10.1109/JESTIE.2021.3066897.

[6] Y. Liu, X. Yang, and X. Wang, "A Compact Inductively Coupled SiC MOSFET Snubber for Quasi-Zero-Voltage Turn-On, Switching Oscillation, and Voltage Spike Suppression," in *IEEE Journal of Emerging and Selected Topics in Power Electronics*, vol. 12, no. 3, pp. 3135-3145, June 2024, doi: 10.1109/JESTPE.2024.3385477.

[7] D. Nair, K. Prasad, and T. Lie, “Standalone Electric Vehicle Charging Station using an Isolated Bidirectional Converter with Snubber,” *Energy Storage*, vol. 3, 2021, doi: 10.1002/est2.255.

[8] M. S. Banjanin and M. S. Savić, "Experimental Registration and Numerical Simulation of the Transient Overvoltages Caused by Single Phase Intermittent Arc Earth Fault in 35 kV Network With Isolated Neutral," in *IEEE Transactions on Power Delivery*, vol. 37, no. 3, pp. 1795-1802, June 2022, doi: 10.1109/TPWRD.2021.3098829.

[9] T. L. Vandoorn, J. De Kooning, B. Meersman, and L. Vandevelde, "Voltage-Based Droop Control of Renewables to Avoid On–Off Oscillations Caused by Overvoltages," in *IEEE Transactions on Power Delivery*, vol. 28, no. 2, pp. 845-854, April 2013, doi: 10.1109/TPWRD.2013.2241793.

[10] M. S. Krishna Reddy, D. Elangovan, Uthra, and R. Saravanakumar, "Analysis design and implementation of VSI fed high gain full bridge isolated DC-DC converter for renewable energy applications," *2013 International Conference on Renewable Energy and Sustainable Energy (ICRESE)*, pp. 45-50, 2013, doi: 10.1109/ICRESE.2013.6927830.

[11] R. Vimala, K. Baskaran, and K. A. Britto, “Characterization of Conducted EMI Generated by Switched Power Converters,” *International Journal of Recent Trends in Engineering*, vol. 1, no. 3, p. 305, 2009.

[12] H. Yeşilyurt and H. Bodur, “New active snubber cell for high power isolated PWM DC–DC converters,” *IET Circuits, Devices & Systems*, vol. 13, no. 6, pp. 822-829, 2019.

[13] H. Nie, X. Liu, Y. Wang, Y. Yao, Z. Gu, and C. Zhang, "Breaking Overvoltage of Dry-Type Air-Core Shunt Reactors and its Cumulative Effect on the Interturn Insulation," in *IEEE Access*, vol. 7, pp. 55707-55720, 2019, doi: 10.1109/ACCESS.2019.2913763

[14] K. Bhatt, R. A. Gupta, and N. Gupta, “Design and development of isolated snubber based bidirectional DC–DC converter for electric vehicle applications,” *IET Power Electronics*, vol. 12, no. 13, pp. 3378-3388, 2019.

[15] Y. Zhang, W. Zhang and J. Yu, "Adaptive Quasi-Three-Level PWM Control Method for Suppressing Overvoltage at Load Coil Terminal of Switching Power Amplifier," in *IEEE Transactions on Industrial Electronics*, vol. 71, no. 7, pp. 7570-7579, July 2024, doi: 10.1109/TIE.2023.3301513

[16] P. E. Tsareva, B. A. Avdeev, N. N. Markovkina, I. R. Epifantsev, and A. A. Zhilenkov, “Simulation of the operation of a three-phase solid-state transformer under variation of load,” *Russian Electrical Engineering*, vol. 93, no. 6, pp. 420-423, 2022.

[17] U. Prasanna and A. K. Rathore, "Small signal analysis and control design of current-fed full-bridge isolated dc/dc converter with active-clamp," *2012 IEEE International Symposium on Industrial Electronics*, pp. 509-514, 2012, doi: 10.1109/ISIE.2012.6237139.

[18] Lalmalsawmi and P. K. Biswas, "Full-Bridge DC-DC Converter and Boost DC-DC Converter with Resonant Circuit For Plug-in Hybrid Electric Vehicles," *2022 International Conference on Intelligent Controller and Computing for Smart Power (ICICCSP)*, pp. 1-6, 2022.

[19] Z. Xing, X. Ruan, H. You, X. Yang, D. Yao, and C. Yuan, "Soft-Switching Operation of Isolated Modular DC/DC Converters for Application in HVDC Grids," in *IEEE Transactions on Power Electronics*, vol. 31, no. 4, pp. 2753-2766, 2016.

[20] M. S. Diab and X. Yuan, "A Quasi-Three-Level PWM Scheme to Combat Motor Overvoltage in SiC-Based Single-Phase Drives," in *IEEE Transactions on Power Electronics*, vol. 35, no. 12, pp. 12639-12645, Dec. 2020, doi: 10.1109/TPEL.2020.2994289.

[21] B. Xiang *et al*., "DC Interrupting With Self-Excited Oscillation Based on the Superconducting Current-Limiting Technology," in *IEEE Transactions on Power Delivery*, vol. 33, no. 1, pp. 529-536, Feb. 2018, doi: 10.1109/TPWRD.2017.2718589.

[22] V. R. K. Kanamarlapudi, B. Wang, N. K. Kandasamy, and P. L. So, "A New ZVS Full-Bridge DC–DC Converter for Battery Charging With Reduced Losses Over Full-Load Range," in *IEEE Transactions on Industry Applications*, vol. 54, no. 1, pp. 571-579, Jan.-Feb. 2018, doi: 10.1109/TIA.2017.2756031

[23] H. Radmanesh, "Distribution Network Protection Using Smart Dual Functional Series Resonance-Based Fault Current and Ferroresonance Overvoltage Limiter," in *IEEE Transactions on Smart Grid*, vol. 9, no. 4, pp. 3070-3078, July 2018, doi: 10.1109/TSG.2016.2626152.

[24] B. Adamczyk, M. Florkowski, and M. Swiatkowski, "Effect of shielding on surge overvoltages in multilayer type windings of power transformer," in *IEEE Transactions on Dielectrics and Electrical Insulation*, vol. 23, no. 3, pp. 1627-1635, June 2016, doi: 10.1109/TDEI.2016.005691.

[25] P. Bhargavi, P. C. V. Chaganti, V. Sowmya, P. V. Manitha, and S. Lekshmi, "A Comparative study of Phase shifted Full Bridge and High-Frequency Resonant Transistor DC-DC Converters for EV Charging Application," *2022 IEEE 2nd International Conference on Mobile Networks and Wireless Communications (ICMNWC)*, pp. 1-6, 2022, doi: 10.1109/ICMNWC56175.2022.10031773.

[26] J. -Y. Lee and J. -H. Jung, "Multi-port DC-DC Converter for Interconnecting Bipolar DC Buses of Bipolar DC Distribution System," *2021 IEEE Energy Conversion Congress and Exposition (ECCE)*, pp. 1191-1196, 2021, doi: 10.1109/ECCE47101.2021.9595214.

[27] S. H. Kung and G. J. Kish, "A Modular Multilevel HVDC Buck–Boost Converter Derived From Its Switched-Mode Counterpart," in *IEEE Transactions on Power Delivery*, vol. 33, no. 1, pp. 82-92, Feb. 2018, doi: 10.1109/TPWRD.2017.2690635

[28] Z. Kan, P. Li, R. Yuan, and C. Zhang, "Interleaved three-level bi-directional DC-DC converter and power flow control," *2018 3rd International Conference on Intelligent Green Building and Smart Grid (IGBSG)*, pp. 1-4, 2018, doi: 10.1109/IGBSG.2018.8393534.

[29] M. Davarpanah, M. Sanaye-Pasand, and F. Badrkhani Ajaei, "CCVT Failure due to Improper Design of Auxiliary Voltage Transformers," in *IEEE Transactions on Power Delivery*, vol. 27, no. 1, pp. 391-400, Jan. 2012, doi: 10.1109/TPWRD.2011.2171511.

[30] N. Schmied, S. Matlok, and M. März, "Analysis of the Zero Overvoltage Switching Phenomenon," in *IEEE Access*, vol. 10, pp. 128263-128275, 2022, doi: 10.1109/ACCESS.2022.3227442.

[31] A. T. Waghe and S. K. Patil, "A bidirectional DC-DC converter fed separately excited DC motor electric vehicle application," *2020 International Conference on Emerging Trends in Information Technology and Engineering (ic-ETITE)*, pp. 1-5, 2020, doi: 10.1109/ic-ETITE47903.2020.421.

[32] A. Ganjavi, H. Ghoreishy, A. A. Ahmad, and Z. Zhagn, "A Three-Level Three-port Bidirectional DC-DC Converter," *2018 IEEE International Power Electronics and Application Conference and Exposition (PEAC)*, pp. 1-4, 2018, doi: 10.1109/PEAC.2018.8590338.

[33] L. Shu *et al*., "A Resonant ZVZCS DC–DC Converter With Two Uneven Transformers for an MVDC Collection System of Offshore Wind Farms," in *IEEE Transactions on Industrial Electronics*, vol. 64, no. 10, pp. 7886-7895, 2017, doi: 10.1109/TIE.2017.2694389.

[34] Z. Wang, L. Pang, T. Wang, H. Yang, Q. Zhang, and J. Li, "Breakdown characteristics of oil-paper insulation under lightning impulse waveforms with oscillations," in *IEEE Transactions on Dielectrics and Electrical Insulation*, vol. 22, no. 5, pp. 2620-2627, 2015, doi: 10.1109/TDEI.2015.005115

[35] M. S. Ansari, A. Shukla, and H. J. Bahirat, "Analysis and Design of MMC-Based High-Power DC–DC Converter With Trapezoidal Modulation," in *IEEE Transactions on Power Electronics*, vol. 38, no. 6, pp. 7256-7270, 2023, doi: 10.1109/TPEL.2023.3249463.

[36] F. A. de Toledo Silva, W. Komatsu, and J. Antonio Jardini, "Use of DC/DC converters modeled as AC-DC converters in HVDC Grids," *2020 IEEE PES Transmission & Distribution Conference and Exhibition - Latin America (T&D LA)*, pp. 1-6, 2020, doi: 10.1109/TDLA47668.2020.9326156.

[37] Y. Hu *et al*., "Ultrahigh Step-up DC–DC Converter for Distributed Generation by Three Degrees of Freedom (3DoF) Approach," in *IEEE Transactions on Power Electronics*, vol. 31, no. 7, pp. 4930-4941, 2016, doi: 10.1109/TPEL.2015.2487821.

[38] N. A. Al-Obaidi, R. A. Abbas, and H. F. Khazaal, "A Review of Non-Isolated Bidirectional DC-DC Converters for Hybrid Energy Storage System," *2022 5th International Conference on Engineering Technology and its Applications (IICETA)*, pp. 248-253, 2022, doi: 10.1109/IICETA54559.2022.9888704.

[39] J. Khodabakhsh and G. Moschopoulos, "A study of multilevel resonant DC-DC converters for conventional DC voltage bus applications," *2018 IEEE Applied Power Electronics Conference and Exposition (APEC)*, pp. 2135-2141, 2018, doi: 10.1109/APEC.2018.8341312.

[40] F. Zhang, W. Li, and G. Joós, "A Transformerless Hybrid Modular Multilevel DC–DC Converter With DC Fault Ride-Through Capability," in *IEEE Transactions on Industrial Electronics*, vol. 66, no. 3, pp. 2217-2226, 2019, doi: 10.1109/TIE.2018.2869355.

[41] R. Dwivedi, S. Singh, B. Singh, A. Chandra, and M. Rezkallah, "Three-Phase AC/DC Converter fed Two Parallel Interleaved DC-DC Converters for Fast Charging Applications with Improved Power Quality," *2023 IEEE 14th International Conference on Power Electronics and Drive Systems (PEDS)*, pp. 1-6, 2023, doi: 10.1109/PEDS57185.2023.10246676.

[42] R. Raju and J. Leonard, "A multi-level AC or DC-DC converter using self-bypassable fixed transfer ratio modules," *2024 IEEE Applied Power Electronics Conference and Exposition (APEC)*, pp. 29-33, 2024, doi: 10.1109/APEC48139.2024.10509094.

[43] H. Silva-Saravia, H. Pulgar-Painemal, L. M. Tolbert, D. A. Schoenwald, and W. Ju, "Enabling Utility-Scale Solar PV Plants for Electromechanical Oscillation Damping," in *IEEE Transactions on Sustainable Energy*, vol. 12, no. 1, pp. 138-147, 2021, doi: 10.1109/TSTE.2020.2985999.

[44] N. Hou and Y. W. Li, "Family of Hybrid dc-dc Converters for Connecting DC Current Bus and DC Voltage Bus," *2020 IEEE Energy Conversion Congress and Exposition (ECCE)*, pp. 412-417, 2020, doi: 10.1109/ECCE44975.2020.9235473.

[45] T. Saha, A. C. Bagchi, and R. A. Zane, "Analysis and Design of an LCL–T Resonant DC–DC Converter for Underwater Power Supply," in *IEEE Transactions on Power Electronics*, vol. 36, no. 6, pp. 6725-6737, 2021, doi: 10.1109/TPEL.2020.3034298.

[46] J. Zeng, X. Du, and Z. Yang, "A Multiport Bidirectional DC–DC Converter for Hybrid Renewable Energy System Integration," in *IEEE Transactions on Power Electronics*, vol. 36, no. 11, pp. 12281-12291, 2021, doi: 10.1109/TPEL.2021.3082427.

[47] H. Wu, Y. Jia, F. Yang, L. Zhu, and Y. Xing, "Two-Stage Isolated Bidirectional DC–AC Converters With Three-Port Converters and Two DC Buses," in *IEEE Journal of Emerging and Selected Topics in Power Electronics*, vol. 8, no. 4, pp. 4428-4439, 2020, doi: 10.1109/JESTPE.2019.2936145.

[48] V. Monteiro, J. C. Tiago Sousa, and J. L. Afonso, "A Novel Topology of Modular Multilevel Bidirectional Non-Isolated dc-dc Converter," *2020 International Young Engineers Forum (YEF-ECE)*, pp. 61-66, 2020, doi: 10.1109/YEF-ECE49388.2020.9171809.

[49] J. Sim, J. Lee, H. Choi, and J. -H. Jung, "High Power Density Bidirectional Three-Port DC-DC Converter for Battery Applications in DC Microgrids," *2019 10th International Conference on Power Electronics and ECCE Asia (ICPE 2019 - ECCE Asia)*, pp. 843-848, 2019, doi: 10.23919/ICPE2019-ECCEAsia42246.2019.8797043.

[50] D. Wang, G. Lebel, C. Gavriluta, and R. Caire, "Impacts of Virtual Primary Frequency Regulation on Electromechanical Oscillations,"

in *IEEE Transactions on Smart Grid*, vol. 9, no. 5, pp. 4270-4281, 2018, doi: 10.1109/TSG.2017.2654198.

[51] S. S. Nag, R. Panigrahi, S. K. Mishra, A. Joshi, K. D. T. Ngo, and S. Mandal, "A Theory to Synthesize Nonisolated DC–DC Converters Using Flux Balance Principle," in *IEEE Transactions on Power Electronics*, vol. 34, no. 11, pp. 10910-10924, 2019, doi: 10.1109/TPEL.2019.2898702.

[52] G. P. Adam, F. Alsokhiry, Y. Al-Turki, M. O. Ajangnay, and A. Y. Amogpai, "DC-DC Converters for Medium and High Voltage Applications," *IECON 2019 - 45th Annual Conference of the IEEE Industrial Electronics Society*, pp. 3337-3342, 2019, doi: 10.1109/IECON.2019.8926872.

[53] J. Li, X. Yang, M. Xu, Y. Ding, L. Wang, and J. Wang, "Investigation on Optimal Switching Oscillation Suppression for SiC MOSFET by Inductively Coupled Damping," in *IEEE Journal of Emerging and Selected Topics in Power Electronics*, vol. 11, no. 1, pp. 667-678, 2023, doi: 10.1109/JESTPE.2022.3213180

[54] K. Tesaki and M. Hagiwara, "A Bidirectional Non-isolated DC-DC Converter Based on Switched-Capacitor Converters for DC Electric Railways," *2020 IEEE Energy Conversion Congress and Exposition (ECCE)*, pp. 613-620, 2020, doi: 10.1109/ECCE44975.2020.9236402.

[55] L. Cai *et al*., "Distribution Characteristics of Induced Overvoltage Along 10 kV Distribution Line Caused by Artificially Triggered Lightning at 40 m," in *IEEE Transactions on Electromagnetic Compatibility*, vol. 66, no. 1, pp. 195-203, 2024, doi: 10.1109/TEMC.2023.3339685

[56] U. Manandhar, H. B. Gooi, X. Zhang, Y. Jian, W. Benfei, and J. Z. Xin, "Dynamic Evolution Control For Three-Level DC-DC Converter with Supercapacitor System," *IECON 2019 - 45th Annual Conference of the IEEE Industrial Electronics Society*, pp. 3883-3887, 2019, doi: 10.1109/IECON.2019.8926660.

[57] D. Zhang, C. Chen, Y. Ou, T. Zheng, and W. Tang, "Model predictive control of three-level bidirectional DC-DC converter based on super capacitor energy storage system," *2020 International Conference on Electrical Engineering (ICEE)*, pp. 1-5, 2020, doi: 10.1109/ICEE49691.2020.9249868.

[58] K. Tesaki and M. Hagiwara, "High-efficiency Operation of a Bidirectional Non-isolated DC-DC Converter Based on Flying-capacitor Converters," *2021 IEEE Energy Conversion Congress and Exposition (ECCE)*, pp. 1981-1988, 2021, doi: 10.1109/ECCE47101.2021.9595773.

[59] B. Wang, W. Peng, G. Feng, X. Zhang, Y. Wang, and U. Manandhar, "Bidirectional Multiple-Port Three-Level DC-DC Converter for HESS in DC Microgrids," *2020 IEEE 18th International Conference on Industrial Informatics (INDIN)*, pp. 609-614, 2020.

[60] V. F. Pires, D. Foito, A. Cordeiro, and A. J. Pires, "A Bidirectional DC-DC Converter to Interlink Unipolar and Bipolar DC Microgrids," *2021 9th International Conference on Smart Grid (icSmartGrid)*, pp. 37-42, 2021, doi: 10.1109/icSmartGrid52357.2021.9551209.

[61] D. S. Ramteke and M. B. Gaikwad, "Isolated DC-DC Converter Fed DC Motor for Bidirectional Electric Vehicular Application," *2018 International Conference on Smart Electric Drives and Power System (ICSEDPS)*, pp. 33-37, 2018, doi: 10.1109/ICSEDPS.2018.8536061.

[62] Y. Zhang, "Analysis of High Gain DC-DC Converters for DC Microgrid," *2023 IEEE 3rd International Conference on Power, Electronics and Computer Applications (ICPECA)*, pp. 1354-1359, 2023, doi: 10.1109/ICPECA56706.2023.10075947.

[63] P. Argo Dahono and A. Dahono, "A Family of Modular Multilevel Bidirectional DC-DC Converters for High Voltage-Ratio and Low-Ripple Applications," *2020 IEEE Energy Conversion Congress and Exposition (ECCE)*, pp. 3934-3940, 2020.

[64] J. Wang *et al*., "Power Flow Calculation for DC Distribution Network Considering DC-DC Converter Control Mode," *2020 IEEE/IAS Industrial and Commercial Power System Asia (I&CPS Asia)*, pp. 385-390, 2020, doi: 10.1109/ICPSAsia48933.2020.9208472.

[65] A. Sweatha, B. Baskaran, and P. Duraipandy, "An Extensive Review of DC-DC Converter Topologies for Water-Pumping Application," *2022 International Conference on Innovations in Science and Technology for Sustainable Development (ICISTSD)*, pp. 151-156, 2022, doi: 10.1109/ICISTSD55159.2022.10010591.

[66] C. Yang, Y. Pei, L. Wang, L. Yu, F. Zhang, and B. Ferreira, "Overvoltage and Oscillation Suppression Circuit With Switching Losses Optimization and Clamping Energy Feedback for SiC MOSFET," in *IEEE Transactions on Power Electronics*, vol. 36, no. 12, pp. 14207-14219, 2021, doi: 10.1109/TPEL.2021.3090031

[67] H. Wu, M. Han, and K. Sun, "Dual-Voltage-Rectifier-Based Single-Phase AC–DC Converters With Dual DC Bus and Voltage-Sigma Architecture for Variable DC Output Applications," in *IEEE Transactions on Power Electronics*, vol. 34, no. 5, pp. 4208-4222, 2019, doi: 10.1109/TPEL.2018.2864584.

[68] Z. W. Khan, H. Minxiao, C. Kai, L. Yang, and A. u. Rehman, "State of the Art DC-DC Converter Topologies for the Multi-Terminal DC Grid Applications: A Review," *2020 IEEE International Conference on Power Electronics, Smart Grid and Renewable Energy (PESGRE2020)*, pp. 1-7, 2020, doi: 10.1109/PESGRE45664.2020.9070529.

[69] S. S. Khan and H. Wen, "A Comprehensive Review of Fault Diagnosis and Tolerant Control in DC-DC Converters for DC Microgrids," in *IEEE Access*, vol. 9, pp. 80100-80127, 2021, doi: 10.1109/ACCESS.2021.3083721.

[70] S. Lu, M. Mu, Y. Jiao, F. C. Lee, and Z. Zhao, "Coupled Inductors in Interleaved Multiphase Three-Level DC–DC Converter for High-Power Applications," in *IEEE Transactions on Power Electronics*, vol. 31, no. 1, pp. 120-134, 2016, doi: 10.1109/TPEL.2015.2398572.

[71] J. Wang, H. Wu, T. Yang, L. Zhang, and Y. Xing, "Bidirectional Three-Phase DC–AC Converter With Embedded DC–DC Converter and Carrier-Based PWM Strategy for Wide Voltage Range Applications," in *IEEE Transactions on Industrial Electronics*, vol. 66, no. 6, pp. 4144-4155, 2019, doi: 10.1109/TIE.2018.2866080.

[72] S. Zhao, Y. Chen, S. Cui, B. J. Mortimer, and R. W. De Doncker, "Three-Port Bidirectional Operation Scheme of Modular-Multilevel DC–DC Converters Interconnecting MVDC and LVDC Grids," in *IEEE Transactions on Power Electronics*, vol. 36, no. 7, pp. 7342-7348, 2021, doi: 10.1109/TPEL.2020.3041721.

[73] Z. Zhang, A. Mallik, and A. Khaligh, "A High Step-Down Isolated Three-Phase AC-DC Converter," in *IEEE Journal of Emerging and Selected Topics in Power Electronics*, vol. 6, no. 1, pp. 129-139, 2018, doi: 10.1109/JESTPE.2017.2725821.

[74] Y. Xiao *et al*., "A Passive Oscillation DC Breaking Scheme Based on Enhanced Vacuum Interrupter," in *IEEE Transactions on Power Electronics*, vol. 37, no. 6, pp. 7344-7353, 2022, doi: 10.1109/TPEL.2021.3131821.

[75] M. W. Beraki, J. P. F. Trovão, M. S. Perdigão, and M. R. Dubois, "Variable Inductor Based Bidirectional DC–DC Converter for Electric Vehicles," in *IEEE Transactions on Vehicular Technology*, vol. 66, no. 10, pp. 8764-8772, 2017, doi: 10.1109/TVT.2017.2710262.

[76] D. Peng, M. Huang, J. Li, J. Sun, X. Zha, and C. Wang, "Large-Signal Stability Criterion for Parallel-Connected DC–DC Converters With Current Source Equivalence," in *IEEE Transactions on Circuits and Systems II: Express Briefs*, vol. 66, no. 12, pp. 2037-2041, 2019, doi: 10.1109/TCSII.2019.2895842.

[77] H. Xiao *et al*., "Analysis of Transient Overvoltage in 220 kV Saturated Core HTS FCL," in *IEEE Transactions on Magnetics*, vol. 47, no. 10, pp. 2620-2623, 2011, doi: 10.1109/TMAG.2011.2158575.

[78] T. Konjedic, L. Korošec, M. Truntič, C. Restrepo, M. Rodič, and M. Milanovič, "DCM-Based Zero-Voltage Switching Control of a Bidirectional DC–DC Converter With Variable Switching Frequency," in *IEEE Transactions on Power Electronics*, vol. 31, no. 4, pp. 3273-3288, 2016, doi: 10.1109/TPEL.2015.2449322.

[79] M. S. Ansari, I. C. Rath, S. K. Patro, A. Shukla, and H. J. Bahirat, "High Power Parallel Hybrid DC-DC Converter," in *IEEE Transactions on Industry Applications*, vol. 59, no. 1, pp. 1077-1089, 2023, doi: 10.1109/TIA.2022.3217026.

[80] W. Sima, Y. Huang, P. Sun, J. Xu, M. Yang, and L. Ye, "Statistical Failure Characteristics of Air Gap Subjected to Damped Alternating Overvoltages and Its Risk Assessment," in *IEEE Transactions on Dielectrics and Electrical Insulation*, vol. 28, no. 3, pp. 797-805, 2021, doi: 10.1109/TDEI.2021.009352.